Adsorption of 2-Mercaptobenzothiazole Organic Inhibitor and its Effects on Copper Anodic Oxidation in Alkaline Environment

Vishant Garg, Sandrine Zanna, Antoine Seyeux, Frédéric Wiame, Vincent Maurice, Philippe Marcus

OPEN ACCESS

Adsorption of 2-Mercaptobenzothiazole Organic Inhibitor and its Effects on Copper Anodic Oxidation in Alkaline Environment

To cite this article: Vishant Garg *et al* 2023 *J. Electrochem. Soc.* **170** 071502

Journal of The Electrochemical Society, 2023 **170** 071502

Adsorption of 2-Mercaptobenzothiazole Organic Inhibitor and its Effects on Copper Anodic Oxidation in Alkaline Environment

Vishant Garg, Sandrine Zanna, Antoine Seyeux, Frédéric Wiame, Vincent Maurice,[z] and Philippe Marcus[*,z]

PSL University, CNRS—Chimie ParisTech, Institut de Recherche de Chimie Paris, Physical Chemistry of Surfaces Research Group, 11 rue Pierre et Marie Curie, 75005 Paris, France

The adsorption of 2-MBT organic inhibitor on copper and its effects on anodic oxide growth in NaOH were investigated using cyclic voltammetry, X-ray photoelectron spectroscopy, and time-of-flight secondary ion mass spectrometry techniques. It is shown that 2-MBT significantly impedes the growth of the Cu(I) oxide by forming a multilayered organic film on the surface. A major factor influencing the formation and properties of the organic barrier layer is the presence and structure of the interfacial native oxide on which it forms. The 2-MBT multilayer bonds to the metallic copper substrate mostly via its sulphur atoms along with a small fraction of the nitrogen atoms also bonding to the metallic substrate. Additionally, there is an interaction between the inhibitor molecules and copper released from the surface to form metal-organic complexes in the outer layers of the thicker films.
 [DOI: 10.1149/1945-7111/ace33b]

Manuscript submitted April 12, 2023; revised manuscript received June 28, 2023. Published July 11, 2023.

Supplementary material for this article is available online

The extensive range of applications of copper metal and its alloys has made it a subject of considerable research in terms of corrosion understanding and prevention. The corrosion of copper is highly dependent on the stability of the oxide layer that naturally forms on the metallic substrate.[1,2] The Pourbaix diagram predicts that, in aqueous environments, this oxide layer, which provides protection by passivation, is only stable at a pH higher than 5.[3] However, numerous other factors can influence the protective properties of the passive film, including its structure and stability.

The oxidation of copper has been studied in detail by several authors.[4–12] Among others, Wiame et al. discussed the initial stages of copper oxidation when copper is exposed to gaseous oxygen at low pressure,[11] while Pinnel et al. studied the effect of temperature and air quality on the growth of copper oxide.[12] Several studies were also performed on the formation of the oxide layers by anodic polarization of the surface in alkaline solutions such as NaOH, KOH, and borate buffer solutions.[4–10] Therefore, the passive oxide film formation, its structure, and its properties are well documented. In alkaline environment, it has been evidenced that copper first oxidizes to form a Cu_2O layer above the copper metal surface upon anodic polarization. This is followed at higher potential by the formation of a $Cu(OH)_2$ and CuO mixed second layer on top of the Cu_2O oxide layer.[6,9,10] These oxide layers are known to protect the copper metal surface from corrosion attack since they physically hinder the access of the corrosive ions to the metal surface, therefore not allowing the electrolyte to directly interact with the metal. However, aggressive species such as chloride ions in high concentrations can still penetrate these oxide layers to interact with the metallic substrate, causing passivity breakdown and the initiation of localized corrosion.[13,14]

2-mercaptobenzothiazole (2-MBT) has been well established as an effective corrosion inhibitor for copper in various media.[15–18] The presence of two sulphur atoms and one nitrogen atom in the molecule aids in bonding with the metal substrate and/or surface oxides, thus forming an organic barrier layer that protects the surface from interaction with the environment.[18–22] Depending on the environmental conditions, 2-MBT exists in its thiol, thione, or thiolate form.[23–25] Density functional theory (DFT) calculations have found that the bonding between the copper surface and the 2-MBT molecules occurs mostly via the two sulphur atoms of the molecule (in thione form) or via the exocyclic sulphur and the nitrogen atom (in thiolate form).[26,27] Nevertheless, the role played by the metallic or oxidized state of the surface, the pH of the solution, and other factors that can influence the bonding mechanism of the molecule to the surface, require further experimental investigation.

In acidic environment, it has been demonstrated that 2-MBT reduces the rate of anodic dissolution of copper metal.[15,28,29] However, since not stable at low pH, the passive oxide film cannot play a significant role in protecting the surface and the 2-MBT layer must form directly on the metallic substrate to protect it.[15] In neutral chloride environment, the 2-MBT layer has been shown to inhibit the growth of copper oxide as well as the corrosion of the metallic substrate.[17,18] However, these works were carried out on copper surfaces covered by an air-formed oxide and therefore the extent of protection offered by the 2-MBT layer to the chloride ions is not ascertained. Previous work on 2-MBT layers on copper in an alkaline environment mostly focused on the local passivation at emergent grain boundaries.[30]

In the present work, we studied the adsorption of 2-MBT and its effects on the anodic oxidation of copper in a strong alkaline medium (0.1 M NaOH solution). Various cathodic pre-treatment methods were applied, either in the presence or absence of the inhibitor in the solution, to modify and control the native oxide-covered Cu surface during the formation of the inhibitor layer. Cyclic voltammetry (CV) tests were performed to determine how the oxide growth is altered by the 2-MBT organic inhibitor layers pre-adsorbed in different pre-treatment conditions. Electrochemical measurements were performed in conjunction with surface analysis by X-ray photoelectron spectroscopy (XPS) and time-of-flight—secondary ion mass spectrometry (ToF-SIMS) to investigate the bonding mechanisms of the 2-MBT molecule to the copper surface, including the role of surface native oxides in the formation of the interface with the inhibitor, the effect of increased exposure time to the inhibitor, the stability of the organic inhibitor layer upon anodic polarisation, and the oxide growth upon anodic polarization.

This work aims to clarify the role of 2-MBT on the anodic oxidation of copper by adsorption of the molecule on a well-controlled metallic surface of copper, and without the presence of chlorides in the solution. The absence of chlorides eliminates their interference in the understanding of the oxidation process in a 2-MBT-containing alkaline solution. Additionally, anodic oxidation is

*Electrochemical Society Fellow.
[z]E-mail: vincent.maurice@chimieparistech.psl.eu; philippe.marcus@chimieparistech.psl.eu

studied in the Cu(I) potential range. This allows us to evaluate the effects of 2-MBT on the oxide layer that forms directly on the bare metallic substrate.

Experimental

Polycrystalline samples obtained from high-purity cast electrolytic tough pitch copper (ETP-Cu) were used for experimental analysis, as in previous work.[15,30,31] The surfaces to be studied were mechanically polished using silicon carbide abrasive papers up to 4000 grit, followed by diamond paste down to 0.25 μm. They were then cleaned ultrasonically for 5 min in successive baths of acetone, ethanol, and ultra-pure water (resistivity $>$ 18.2 MΩ.cm). Electrochemical polishing was performed using a 60% orthophosphoric acid (H_3PO_4) solution at a constant voltage of 1.4 V versus a copper counter-electrode for 4 min. This was done to remove the cold-work layer leftover from mechanical polishing.[32] Finally, the samples were rinsed with a 10% solution of H_3PO_4, followed by ultra-pure water, and dried using nitrogen.

The electrochemical experiments were performed using Kel-F (PCTFE) cells containing approximately 350–400 μl of the electrolyte. They were equipped with counter and pseudo-reference electrodes made of platinum. The cells were thoroughly cleaned prior to each experiment as described elsewhere.[9,15] The Pt pseudo-reference was calibrated before each experiment (+0.32 V vs SHE). The working electrode area was 0.16 cm^2, delimited by an O-ring. The experiments were performed using a PicoStat bi-potentiostat and Picoscan software from Agilent Technologies. The electrolytes used for the experiment were a reference 0.1 M NaOH aqueous alkaline solution of pH 13.5 without the inhibitor, and a 0.1 M NaOH +1 mM 2-MBT aqueous solution of pH 13.6 as the solution with inhibitor. All the chemicals used were supplied by Sigma Aldrich and were of analytical grade.

Cathodic pre-treatment was performed prior to the experiments in order to reduce the surface native oxide film. This was done in (a) the absence of 2-MBT, or in (b) the presence of 2-MBT in the solution. After immersion at the open circuit potential (OCP), the potential was swept cathodically, with a scan rate of 20 mV s^{-1}, to the onset of hydrogen gas evolution (–0.90 V vs SHE) and then swept back up to the value of –0.45 V vs SHE. This was repeated 2 more times. For the substrate pre-treated in absence of 2-MBT, the reference NaOH solution was replaced with a 2-MBT containing NaOH solution after the 3rd cathodic pre-treatment cycle. A pipette was used to remove 3/4 of the solution in the cell (approx. 250–300 μl), and subsequently an equal amount of the 2-MBT containing solution was introduced while the substrate and the electrodes of the cell remained immersed and connected. This process was repeated 7 times to ensure that the replaced solution in the cell had the appropriate concentration of 2-MBT. Following this, the substrates were exposed in the 0.1 M NaOH +1 mM 2-MBT solution for either 2 min or 1 h, at a fixed potential of –0.45 V vs SHE, before initiating the anodic oxidation tests.

The anodic oxidation tests were performed by sweeping the potential from –0.45 up to +0.10 V vs SHE, followed by reverse sweeping to –0.90 V vs SHE, and then back to –0.45 V vs SHE with a scan rate of 20 mV s^{-1}. The experimental process from cathodic pre-treatment to the anodic oxidation tests is shown in Fig. 1. The electrochemical experiments were repeated 3 times each to ensure reproducibility.

Surface analysis was performed in the cathodically reduced state of the interface (reduced state at –0.45 V vs SHE), and in the anodically polarized state (anodic state at 0.10 V vs SHE). Once the desired electrochemical state was achieved, the cell was disconnected, the samples rinsed with ultra-pure water, dried using nitrogen, and transferred within less than 2 min for analysis by XPS and ToF-SIMS. The experimental conditions performed to achieve the reduced state and anodic state are summarized in Fig. 1.

XPS analysis was performed with a Thermo Electron Escalab 250 Xi spectrometer of base pressure less than 10^{-10} mbar. A monochromated Al Kα X-ray source (hv = 1486.6 eV) with an X-ray spot size of 900 μm in diameter was used. High-resolution spectra of the C 1s, O 1s, N 1s, S 2p, Cu 2p core levels and Cu LMM Auger transition were recorded with a pass energy of 20 eV at a step size of 0.1 eV at 90° take-off angle of the collected photoelectrons. Curve fitting of the spectra was performed with the Thermo Fischer scientific software Avantage using an iterative Shirley-type background subtraction. CasaXPS software was used to decompose the Cu LMM Auger spectra. The values of the photoionization cross-sections at 1486.6 eV were taken from the Scofield database,[33] the transmission function of the analyser was given by Thermo Fisher, and the inelastic mean free paths were determined using the TPP-2M formula.[34] The binding energies are referred to the Fermi level of the sample.

ToF-SIMS analysis was performed using a ToF-SIMS 5 spectrometer (IonTof—Münster Germany) of base pressure of 5×10^{-9} mbar. SurfaceLab software v6.5 was used for data acquisition and post processing analysis. High current (HC) bunched mode was used for performing analysis using Bi^+ primary ions of 25 keV energy at a target current of 1.2 pA over an area of 100 $\times$ 100 μm^2. Depth profiles were obtained by interlacing analysis in static SIMS conditions with sputtering using a Cs^+ ion gun of 0.5 keV delivering a 20 nA target current over a 500 $\times$ 500 μm^2 area. Both ion beams were at an incidence angle of 45° with respect to the sample surface and well-aligned to ensure analysis at the centre of the sputtered crater. All the acquisitions were done in negative polarity allowing us to analyse both the organic and inorganic regions of the surface layers. The depth profiles were recorded at three separate regions on the surface of each sample to ensure reproducibility.

Results and Discussion

CV analysis of 2-MBT effects on native oxide film reduction and anodic surface oxidation.—Three cycles of cathodic pre-treatment were applied by cyclic voltammetry in order to reduce the native oxide film formed on the copper substrate following surface preparation. The three pre-treatment CVs obtained in the 0.1 M NaOH reference solution are shown in Fig. 2a, and those obtained in a 0.1 M NaOH +1 mM 2-MBT solution in Fig. 2b, with the current density measured as the potential is swept cathodically and back.

For the experiment in the NaOH reference solution (Fig. 2a), a very high negative current with a peak at –0.57 V vs SHE is observed in the first cathodic pre-treatment cycle, corresponding to a large quantity of native Cu_2O being reduced. The measured cathodic charge density was 2311 ± 192 $\mu C\ cm^{-2}$ and the corresponding equivalent thickness of the reduced native oxide film was 2.9 ± 0.2 nm, estimated using Faraday's law,[35] where the molar volume (V_M) of Cu_2O is 23.9 cm^3/mol and the number of electrons exchanged (z) per Cu_2O molecule is 2. The next two cycles of cathodic pre-treatment show negligible cathodic charge densities with no distinct cathodic reduction peak in the potential range where the reduction of the native oxide is expected, suggesting that most of the native oxide film initially formed on the copper surface has been reduced during the first cathodic pre-treatment cycle. Noteworthy is that prior to the first cycle, when the sample is exposed to the 0.1 M NaOH solution at OCP, oxidation of the surface occurs due to the high pH of the solution. This could contribute to a large fraction of the initial oxides measured by electro-reduction.

For the cathodic pre-treatment with 2-MBT present in the NaOH solution (Fig. 2b), we observe that the cathodic current of the first pre-treatment cycle, forming a peak shifted at –0.62 V vs SHE, is much lower than in the absence of the inhibitor. The cathodic charge density was measured to be 937 ± 124 $\mu C\ cm^{-2}$ and the equivalent thickness of reduced Cu_2O was 1.2 ± 0.2 nm, a decrease by a factor of 2.5 compared to the oxide reduced in absence of 2-MBT. It is suggested that the 2-MBT molecules are adsorbed on the oxide film surface already at OCP, forming an organic layer that hinders the reduction reactions.[30] This hindering effect is supported by the lower

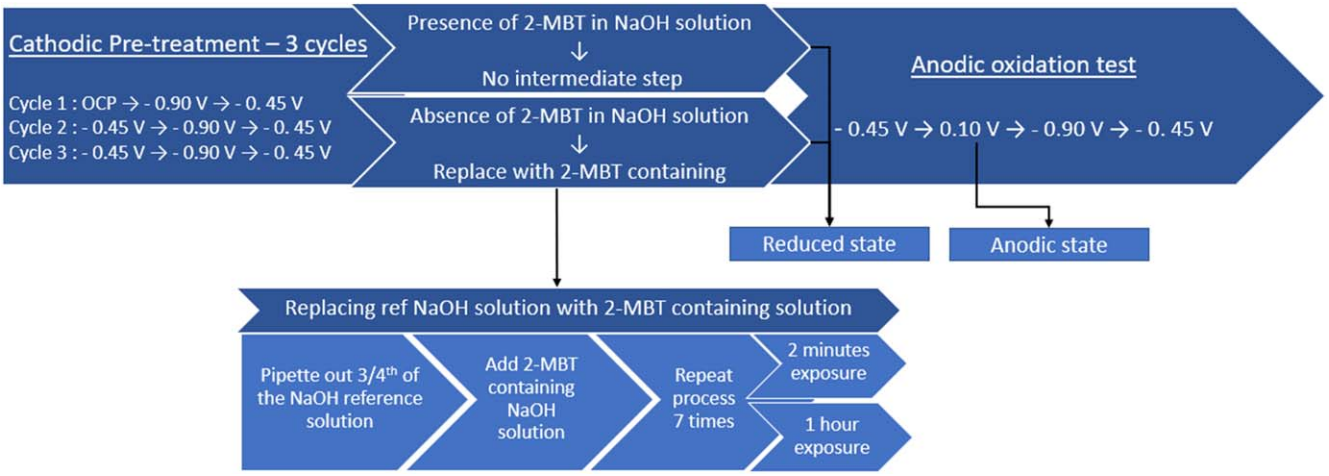

Figure 1. Schematic showing the experimental procedure for the cathodic pre-treatment methods and the anodic oxidation test.

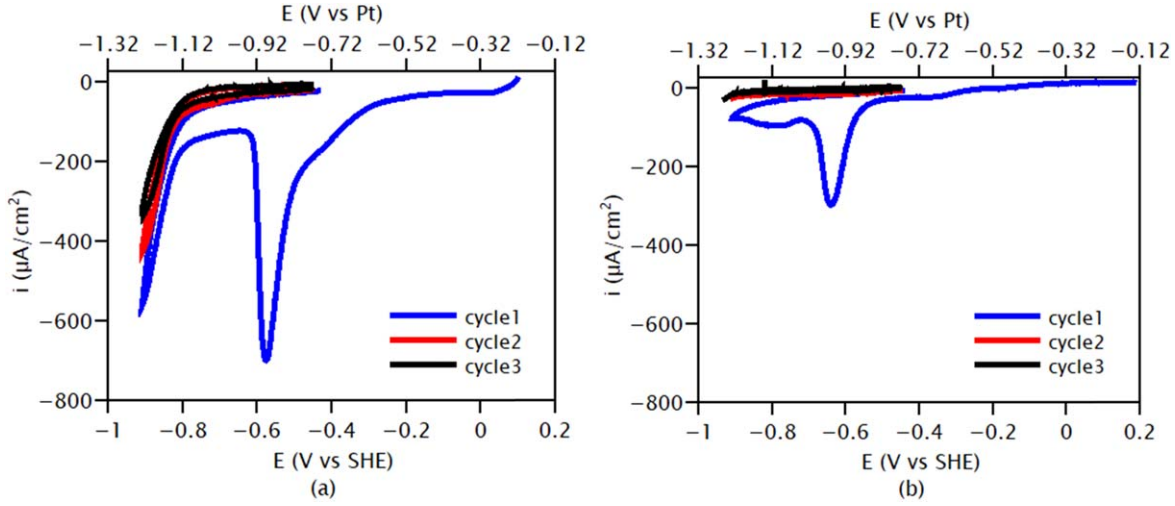

Figure 2. Cathodic pre-treatment CVs for copper in (a) 0.1 M NaOH reference solution (no inhibitor), and (b) 0.1 M NaOH +1 mM 2-MBT solution (with inhibitor). Scan rate is 20 mV s^{-1}.

cathodic current measured in the presence of 2-MBT in the potential range (from OCP to about –0.3 V vs SHE) preceding the reduction of Cu_2O, as well as by the negative shift of the Cu_2O reduction peak. Alternatively, it is possible that upon exposure to the 2-MBT + NaOH solution, the oxide film growth is restricted at OCP conditions due to the interaction of 2-MBT with the surface. Therefore, the lower cathodic current measured could be due to the electro-reduction of the thinner film present in this case. We also observe that the evolution of hydrogen gas does not occur by this pre-treatment method at the potential –0.8 V vs SHE, unlike that observed for the pre-treatment in absence of the inhibitor. This again indicates the hindering effect of 2-MBT on the cathodic reactions within this potential range and is consistent with 2-MBT behaving as a mixed inhibitor (anodic and cathodic).[36]

The next two cycles of cathodic pre-treatment performed in presence of the inhibitor show negligible measured cathodic current densities, indicating that either the oxides are completely reduced or that the reduction of the oxide film is blocked due to the presence of 2-MBT on the surface. Consequently, much more Cu(I) oxide subsists at the interface after pre-treatment in the presence than in the absence of 2-MBT in the NaOH solution, as confirmed by surface analysis discussed hereafter.

The CVs for anodic oxidation performed after varying the pre-treatment conditions of the interface are shown in Figs. 3a–3d. Figure 3a corresponds to the test done in the 0.1 M NaOH reference solution. The other three CVs correspond to the tests performed in presence of 1 mM 2-MBT in the 0.1 M NaOH solution, performed after cathodic pre-treatment in the absence of 2-MBT followed by 2 min (Fig. 3b) and 1 h (Fig. 3c) of exposure to the inhibitor solution at –0.45 V vs SHE, and after cathodic pre-treatment in the presence of 2-MBT (Fig. 3d). The conditions of the interface formation are similar to those studied in previous work on copper in acidic conditions.[15] The charge densities (anodic and cathodic) for each experiment were determined by integrating the current densities with respect to time, and the equivalent thickness of oxide grown during polarization was determined from the cathodic charge density, assuming that (a) the entire anodic charge corresponds only to oxide grown during the experiment and (b) that all the oxides formed during the anodic branch of the CV are reduced during the cathodic branch of the CV. The results are presented in Table I along with the standard error of the measurements.

It is observed that for the solution with no inhibitor, Fig. 3a, oxidation initiates at around –0.40 V vs SHE, with the Cu(I) anodic peak measured at approximately –0.05 V vs SHE. This rise in current density corresponds to the formation of Cu_2O oxide, as observed by others.[4,6–8,30] The initial small feature at approximately –0.30 V vs SHE, prior to the oxidation of the surface, has been associated to the adsorption of OH^- ions,[7,8] possibly forming the soluble $Cu(OH)_2^-$ species.[4] Polarization beyond the potential of 0.05 V vs SHE leads to further oxidation in the Cu (II) range to form

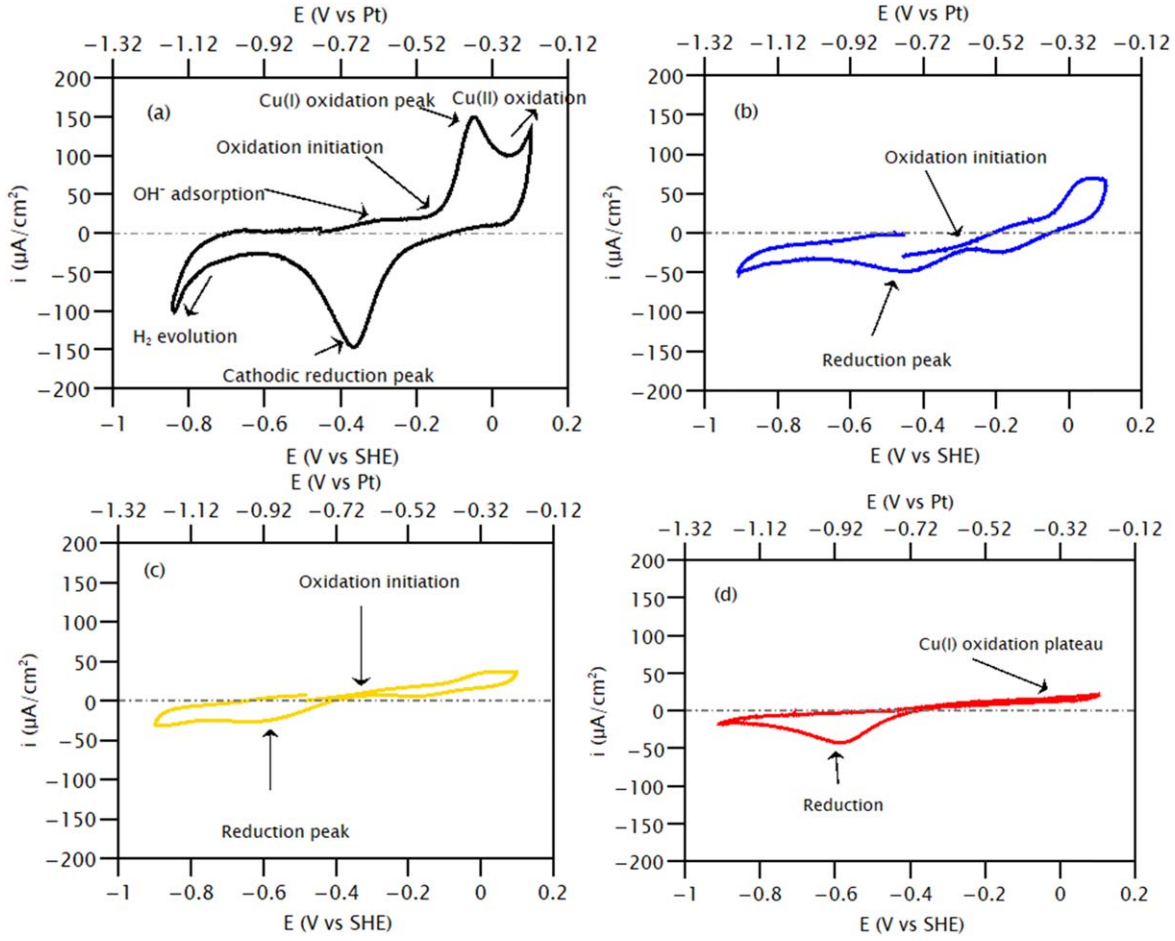

Figure 3. Anodic oxidation CVs for copper in (a) 0.1 M NaOH reference solution following pre-treatment without 2-MBT, and in 0.1 M NaOH +1 mM 2-MBT solution following (b) pre-treatment without 2-MBT and 2 min exposure to 2-MBT, (c) pre-treatment without 2-MBT and 1 h exposure to 2-MBT, and (d) pre-treatment with 2-MBT. Scan rate is 20 mV s^{-1}.

$Cu(OH)_2$ and CuO, as observed by additional experiments and in previous works.[4–10,37] During the cathodic sweep, a single cathodic peak is obtained at –0.36 V vs SHE which indicates the conversion of Cu_2O oxide back to Cu(0) metallic copper. After the potential reaches –0.8 V vs SHE, a sharp increase in the negative current density is observed which corresponds to H_2 evolution.[38]

The CV performed after pre-treatment without 2-MBT following 2 min of exposure to the inhibitor (Fig. 3b) exhibits a lower current density in the Cu(I) oxidation range compared to the reference solution CV (Fig. 3a). The increase in the current density starts at a potential of –0.31 V vs SHE, and the oxidation peak is shifted positively to approximately 0.05 V vs SHE. It is proposed that, in the absence of residual native oxides, an organic film of 2-MBT molecules is formed on the metallic substrate surface exposed to the 2-MBT-containing solution at –0.45 V vs SHE. However, the exposure time of 2 min is too short to complete the formation of an organic barrier film efficiently blocking surface oxidation during subsequent anodic polarization. The organic layer formed in these conditions is likely locally defective, or would break down locally upon polarization, thus allowing for the growth of anodic oxide. The barrier effect is supported by the positive shift of the oxidation peak still observed in the Cu(I) range and by the lower thickness of oxide film grown compared to the reference solution CV (by a factor of approximately 1.5), as seen in Table I.

Like for the experiment reported in Fig. 3b, performing the Cu(I) oxidation test in the 2-MBT-containing solution after cathodic pre-treatment in absence of 2-MBT followed by 1 h of exposure to the inhibitor (Fig. 3c) results in anodic Cu(I) oxidation starting at around –0.31 V and peaking at approximately 0.05 V vs SHE. However, in this case, the current density increase is slightly reduced, indicating higher hindrance to oxide growth. This suggests that the increase in exposure time to 2-MBT allows for the completion of a less defective organic barrier layer, possibly more resistant to break-down, and thus more effective in blocking anodic activity.

For the test performed in the 2-MBT-containing solution and after cathodic pre-treatment in the presence of 2-MBT (Fig. 3d), a much lower anodic activity is observed, without any peak of Cu(I) oxidation. The low rise of anodic current indicates that even though it is significantly reduced, oxidation still occurs on the surface leading to the formation of copper oxides, as attested by the cathodic reduction peak measured at –0.58 V vs SHE on the subsequent reverse scan. The significant reduction in the anodic charge density is by a factor of approximately 2.6 compared to the reference solution CV (Fig. 3a), and by a factor of 1.5 compared to the CV performed after pre-treatment in absence of 2-MBT followed by 1 h exposure to 2-MBT (Fig. 3c), as seen in Table I. This inhibition of the anodic activity agrees with previous work on the effect of 2-MBT on copper passivation.[30] This is assigned to the barrier layer of organic molecules and metal-organic complexes formed by 2-MBT on the residual interfacial layer of native oxide which stabilizes the interface by impinging anodic oxide growth in the Cu(I) potential range.[16,39]

Surface analysis of 2-MBT-covered oxidized interface.—The ToF-SIMS elemental depth profiles of the interfaces obtained after cathodic pre-treatment in the absence of 2-MBT in the solution followed by 1 h of exposure to 2-MBT, and after cathodic pre-treatment in the presence of 2-MBT in the solution, are presented in

Table I. Anodic and cathodic charge densities determined from the anodic oxidation tests along with the equivalent thickness of oxide film grown during the anodic oxidation test and determined from the cathodic charge density.

Exp.	Electrolyte, Pre-treatment	Anodic charge (μC/cm^2)	Cathodic charge (μC/cm^2)	Equivalent thickness of oxide film grown (nm)
a	0.1 M NaOH ref Pre-treatment w/o 2-MBT	1409 ± 10	1252 ± 5	1.55 ± 0.01
b	0.1 M NaOH + 1 mM 2-MBT, Pre-treatment w/o 2-MBT, 2 min exposure to 2-MBT	937 ± 51	779 ± 7	0.96 ± 0.01
c	0.1 M NaOH + 1 mM 2-MBT, Pre-treatment w/o 2-MBT, 1 h exposure to 2-MBT	799 ± 28	356 ± 6	0.44 ± 0.01
d	0.1 M NaOH + 1 mM 2-MBT, Pre-treatment with 2-MBT	537 ± 1	514 ± 1	0.64 ± 0.01

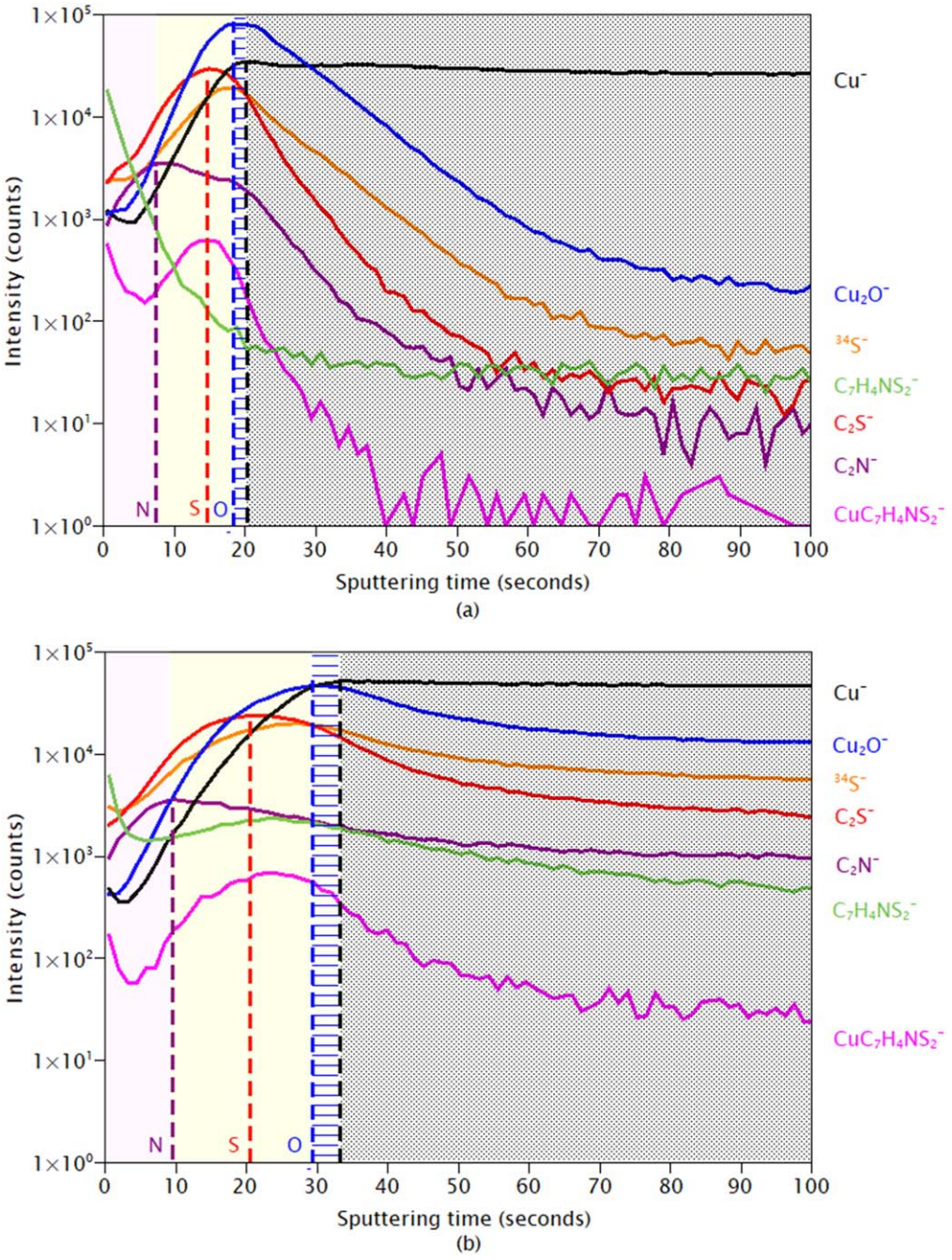

Figure 4. ToF-SIMS depth profiles of the inhibiting interfaces obtained in reduced state after (a) cathodic pre-treatment in the absence of 2-MBT followed by 1 h of exposure to 2-MBT and, (b) cathodic pre-treatment in the presence of 2-MBT.

Figs. 4a, 4b. They display the intensity of the selected secondary ions in logarithmic scale vs the sputtering time, which relates to the depth from the top surface.

Like in recent works,[15,17] the Cu^- and Cu_2O^- ions were selected as characteristic of the metal substrate and metal oxide, respectively, and the $C_7H_4NS_2^-$, C_2N^-, C_2S^-, and $^{34}S^-$ ions as representative of the 2-MBT molecule and its molecular fragments of nitrogen and sulphur, and overall sulphur, respectively. Lastly, the $CuC_7H_4NS_2^-$ ions were selected as characteristic of the Cu-2-MBT interaction, both as bonding on the metallic/oxidized substrate and possible metal-organic complexes. The positions of each layer was defined by the maximum intensity of the corresponding ions with an uncertainty of 5%.

For the depth profile obtained at the reduced state after pre-treatment in the absence of 2-MBT followed by 1 h exposure to 2-MBT (Fig. 4a), the interface with the metallic copper substrate is observed at 20 s of sputtering time, based on the position at which the Cu^- ions profile reaches its maximum intensity. Slower decay of the intensities is observed for all secondary ions in the substrate region, suggesting roughening of the interface. The maximum intensity of the Cu_2O^- ions profile is seen at 18 s of sputtering time, confirming that some copper oxide remains from the native oxide film, although very thin, on the metallic substrate. Similar to previous work,[15] we observe that the intensity of $C_7H_4NS_2^-$ ions is maximum at the topmost surface, followed by the C_2N^- ions and the C_2S^- ions, respectively. This is consistent with 2-MBT forming multilayers, as seen by deposition of 2-MBT in vapour phase[20–22] as well as in neutral aqueous solution,[17] with the innermost layer chemically bonded to the partial oxide-covered surface via the sulphur atoms of the molecule and the outer layers physisorbed on

the surface. The maxima of the $^{34}S^-$ ions is deeper than that of the C_2S^- ions and much closer to the metallic substrate suggesting that there are regions where sulphur (both from the molecule and free dissociated sulphur) is directly bonded to metallic copper in the non-oxide-covered regions of the surface. This is attested by the fact that the maximum of the Cu_2O^- profile occurs nearly at the same depth as that of the $^{34}S^-$ ions, indicating that instead of a complete layer, the oxides are present as islands which are distributed on the surface, which thus enables the sulphur to bond directly to the metal.

The $CuC_7H_4NS_2^-$ ion profile, of which the maximum intensity is observed between the C_2S^- and $^{34}S^-$ ion profiles, indicates that the 2-MBT molecules of the inner layer bond to both metallic and oxidised Cu. The higher intensity of the $CuC_7H_4NS_2^-$ ions observed at the topmost surface also indicates bonding between the molecules and Cu in the outermost layers of the multilayer organic film, most likely forming Cu-2-MBT metal-organic complexes. This is also evidenced in the Cu^- ion profile, where a slightly higher intensity for the initial 4 s of sputtering time is observed, in agreement with the profile of $CuC_7H_4NS_2^-$ ions, indicating an interaction between the Cu ions and the 2-MBT molecule. Although observed in different conditions, the formation of metal-organic complexes can be inferred from the observation of Cu-2-MBT complexes reported previously.[16,39–41]

In reduced state obtained after pre-treatment in the presence of 2-MBT (Fig. 4b), the interface with the Cu metal region is at 34 s of sputtering time, indicating that the covering oxide and organic layers are markedly thicker in this case. Regarding the interfacial oxide, its presence is supported by the maximum intensity of the Cu_2O^- ion profile measured at 29 s, which is at a longer sputtering time from the maximum of the Cu^- ions (characteristic of the metallic Cu) than in the previous case, demonstrating that the remaining copper oxide film or islands are much thicker in this case. Regarding the organic multilayer, it is also thicker than in the previous case according to the larger width of the corresponding region, as indicated by the $CuC_7H_4NS_2^-$ and the $C_7H_4NS_2^-$ profiles. The sequence of the intensity maxima of the depth profiles indicates that it is similarly structured with the inner layer primarily interacting with the partial oxide-covered surface via the S atoms of the molecules and the physically adsorbed outer layers as multilayers and/or bonded to Cu to form metal-organic complexes, as mentioned above. However, for the $C_7H_4NS_2^-$ profile, a small increase in intensity is observed in the inner 2-MBT chemisorbed layer, unlike the previous case, which is most likely representative of the Cu-2-MBT complexes that could be present in this region. Although the $CuC_7H_4NS_2^-$ ion profile exhibits this increase as well in the inner layer, it cannot be completely resolved since the $CuC_7H_4NS_2^-$ ion profile is characteristic of both the bonding on the metallic/oxidized substrate and the metal-organic complexes.

The Cu LMM Auger spectra obtained in reduced and anodic states after pre-treatment in the absence or presence of the inhibitor are shown in Fig. 5. They were decomposed in order to determine the contributions of the Cu(0) and Cu(I) components, corresponding to copper metal and copper oxide respectively, and thus to evaluate the effects of the pre-treatment methods on the presence of interfacial oxides. The decomposition was done by least square fitting, using as components the 2 line-shapes measured, in same analytical conditions, on metallic copper and on oxidized copper reference (Cu_2O thick film) samples, like previously done.[15,22,42,43]

Figures 5a, 5b shows the contributions of the Cu(0) and Cu(I) components obtained after pre-treatment in the absence of 2-MBT followed by 1 h exposure to 2-MBT at the reduced state and anodic state.

It is observed that the intensity of the Cu(I) component is very low here, with the Cu(I)/Cu(0) intensity ratios 0.07 ± 0.01 and 0.05 ± 0.01 for the reduced state and the anodic state, respectively. This low intensity of the component corresponding to Cu(I) oxide indicates that the pre-treatment method is effective in both reducing the native oxides and allowing for the inhibitor molecules to form a dense and protective barrier layer. As seen from the CV tests in Fig. 3c, this barrier layer impedes the formation of Cu(I) oxide in large quantities upon anodic polarization. It also prevents re-oxidation of the sample during transfer through air that would occur in the defective regions of the barrier layer, like observed for 2-MBT layers deposited from the gas phase and imperfectly protecting against re-oxidation.[20] In fact, we observe a minimal decrease, if at all considering the margin of error, for the Cu(I)/Cu(0) intensity ratio in the anodic state of the interface, whereas the CV data shows an increase in current density upon polarization indicating oxidation of the surface (Fig. 3c). A possible explanation is that, in the reduced state, a fraction of the defective areas of the thin 2-MBT barrier layer are re-oxidized in air which then leads to a slightly higher intensity of the Cu(I) component, whereas after anodic polarization these defective sites may be covered by the inhibitor, which would protect them from re-oxidation. This will also be discussed in detail later.

On the samples pre-treated in the presence of the inhibitor molecule, Figs. 5c, 5d, it is observed that despite the reduction of the native oxides by cathodic pre-treatment, a large quantity of Cu(I) ions subsists at the interface resulting in much thicker oxide islands than in the previous case, supporting our hypothesis that the presence of 2-MBT during pre-treatment hinders the reduction of the native oxide film present on the surface. In Fig. 5d, after polarization of the surface, there is a minimal increase in the intensity of the Cu(I) component with the Cu(I)/Cu(0) intensity ratio increasing from 0.72 (±0.03) to 0.77 (±0.03). This agrees with the CV data in Fig. 3d, where a slight increase in current density is seen upon anodic polarization. Although relatively thick, as shown by ToF-SIMS and confirmed below, the organic layer would not fully block anodic oxidation of the surface. This residual growth could occur in the more reactive local areas of the interface, i.e. those initially fully reduced after pre-treatment with no subsisting native oxide film. This view is supported by the quantitative analysis presented below.

It is important to note that a fraction of the Cu(I) intensity can arise from the contribution of the Cu-2-MBT complex, since the state of the copper ions in this complex is suggested to be Cu(I).[16] This is most likely why we obtain such a high intensity for the Cu(I) component in the reduced state obtained after pre-treatment in the presence of 2-MBT. However, we cannot distinguish the Cu(I) ions related to the complex from the Cu(I) ions related to the oxide matrix. Therefore, the O 1s spectrum is studied below to further resolve this issue.

Figure 6 shows the XPS S 2p, N 1s, C 1s, and O 1s core level spectra for the reduced states obtained after pre-treatment in the presence and absence of 2-MBT. The curves were decomposed using the peak components parameters defined in previous work,[15] with an uncertainty of ±0.1 eV for the binding energy values.

In both cases, three components were observed for the S $2p_{3/2}$: S1 at 164.2 eV, S2 at 162.8 eV, and S3 at 161.9 eV. They correspond to endocyclic sulphur of 2-MBT, exocyclic sulphur of 2-MBT, and sulphur bonded directly to metallic Cu respectively, with sulphur from S1 and S2 components not bonded to metallic Cu. This is in agreement with previous work of 2-MBT adsorption in aqueous and vapour phase on Cu.[15,17,20–22]

The N 1s spectra contain two components: N1 at 399.4 eV corresponding to nitrogen from the molecule not bonded to metallic Cu,[15,18,21] and N2 at 398.2 eV corresponding to a direct bonding between N and Cu.[20] This N2 component is a very small fraction compared to the N1 component (less than 5% of the overall nitrogen intensity), indicating that the quantity of nitrogen atoms of the molecule bonding to the metallic substrate is negligible for quantitative analysis. However, this does show that nitrogen, even though only a very small fraction, does bond directly to metallic Cu.

As for the C 1s spectra, they were decomposed into three peaks: C1 at 286.6 eV corresponding to C=S bonds, C2 at 285.6 eV for C-S and C-N bonds, and C3 at 284.8 eV corresponding to C-C and C-H bonds.[20,28] The C1:C2:C3 intensity ratio was determined to be 1:2:4 indicating that the 7 carbon atoms fitted the 2-MBT molecule stoichiometry.[15,20] However, this was not the case for the

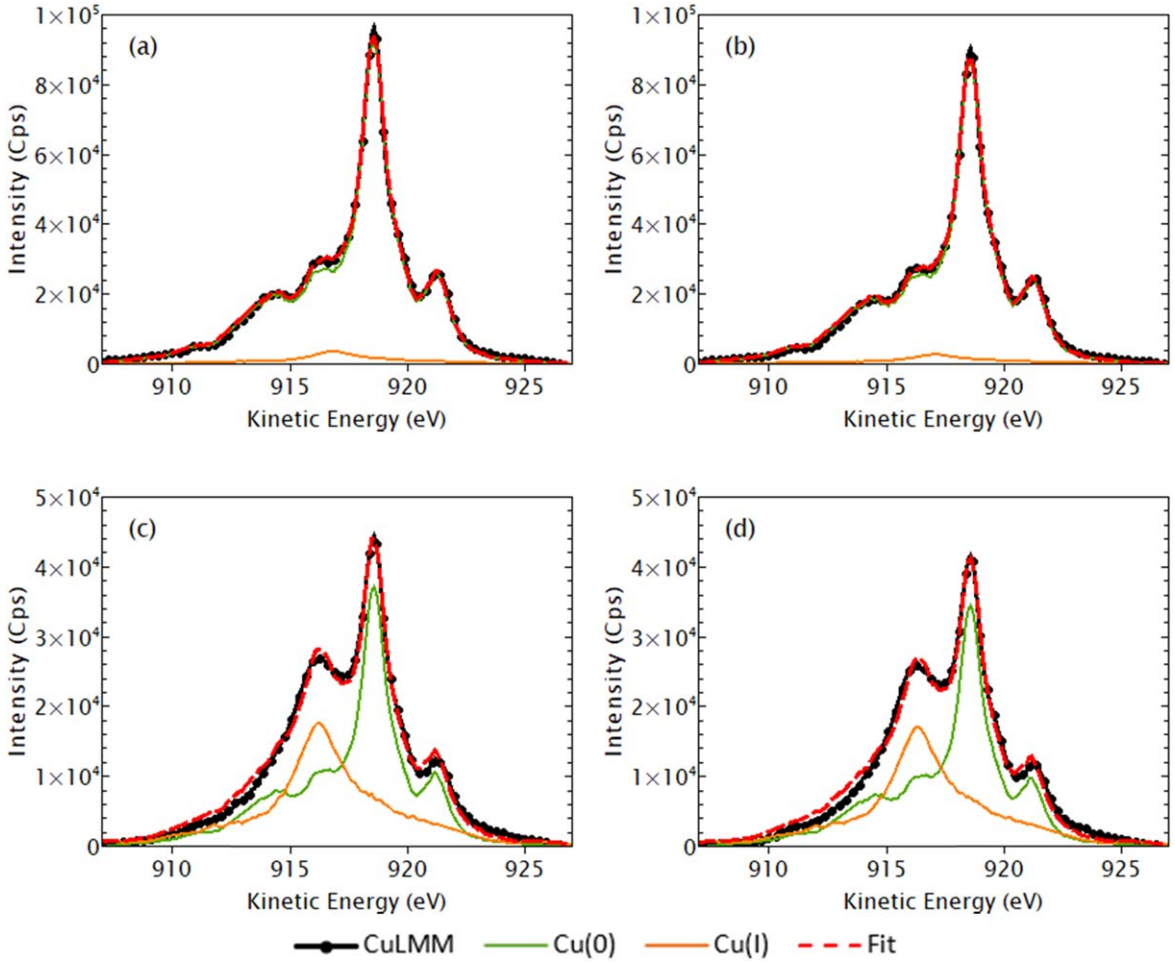

Figure 5. Cu LMM Auger spectra for copper exposed to 0.1 M NaOH+ 1 mM 2-MBT solution at the (a) reduced state, (b) anodic state after cathodic pre-treatment in the absence of 2-MBT followed by 1 h of exposure to 2-MBT, and at the (c) reduced state, (d) anodic state after cathodic pre-treatment in the presence of 2-MBT.

experiment performed after pre-treatment in absence of 2-MBT followed by 1 h exposure to the inhibitor solution, for which we observed an increased intensity at the binding energy of the C1 component (286.6 eV) attributed to an additional C4 component with an FWHM of 1.3 ± 0.1 (+0.2 eV compared to the C1 component). The presence of this C4 component is likely due to the formation of alcohols and/or ethers during the 1-hour exposure to the 0.1 M NaOH +1 mM 2-MBT electrolyte. Since their binding energies are very close to each other, 286.5 eV for alcohols and 286.4 eV for ethers,[44,45] it is difficult to distinguish which group is formed.

Three components were observed from the decomposition of the O 1s spectrum for both sets of experiments. The O1 component at 532.9 eV was assigned to oxygen adsorbed on the surface from water.[21,22,46] The O2 component at 531.4 eV corresponds to hydroxides formed on the surface.[22,42] Lastly, the O3 component at 530 eV was assigned to the Cu(I) oxide present.[21,42,46] A positive shift in BE of 0.5 eV is observed for the O2 and O3 components after pre-treatment in presence of 2-MBT. Several authors have reported varying values of binding energies for the oxygen peaks in the O 1s spectrum relating to the oxide and hydroxide components, ranging from 529.6 to 530.6 eV for the oxide (O3) component and between 530.8 to 531.5 eV for the hydroxide (O2) component.[17,18,20,22,43,46,47] It is found that there is a correlation between the thickness of the oxide layer and the BE values reported, i.e. when the oxide is very thin (∼0.2 nm) the BE is lower and increases with the oxide thickness (up to 1.5 nm). Additionally, previous work shows that when the oxide thickness was between 0.2 to 0.4 nm, the BE for the oxide component was 530.2 ± 0.1 eV.[15] Hence, we can make the argument that the positive shift in BE for the O2 and O3 components here are most likely due to the presence of a thicker oxide layer/islands in this case (pre-treatment with 2-MBT), as evident from the differences in intensity between the O3 peaks of the O 1s spectra. While the shift can also be due to a change in the structure of the oxide layer and its composition, we do not have any evidence of the phenomenon, both experimentally and from literature.

Although observed for both experiments, the O1 component after pre-treatment in the absence of 2-MBT followed by 1 h exposure to the 2-MBT + NaOH solution was much higher (blue curve). This phenomenon correlates to the C4 component of the C 1s spectrum of the same experiment, as mentioned above. However, in this case too, the binding energies of the two functional groups are too close to decompose, 532.9 ± 0.2 eV for alcohols and 532.7 ± 0.2 eV for ethers.[44,48] Therefore, the atomic ratio of the C4 component from the C 1s spectrum and the O1 component of the O 1s spectrum was determined to give a more accurate representation of the species observed here. The atomic ratio for the C4/O1 intensities was found to be 2.54 ± 0.03, indicating that other than the adsorbed oxygen, this species also corresponds to one oxygen atom bonded to either two carbon atoms and/or three carbon atoms. Hence, the C4 component for the reduced state after pre-treatment in the absence of 2-MBT followed by 1 h exposure to 2-MBT is assigned to the formation of ethers due to an interaction of the hydroxide ions with carbon from either the 2-MBT molecule or from contamination. Angle resolved measurements confirmed that this species is formed

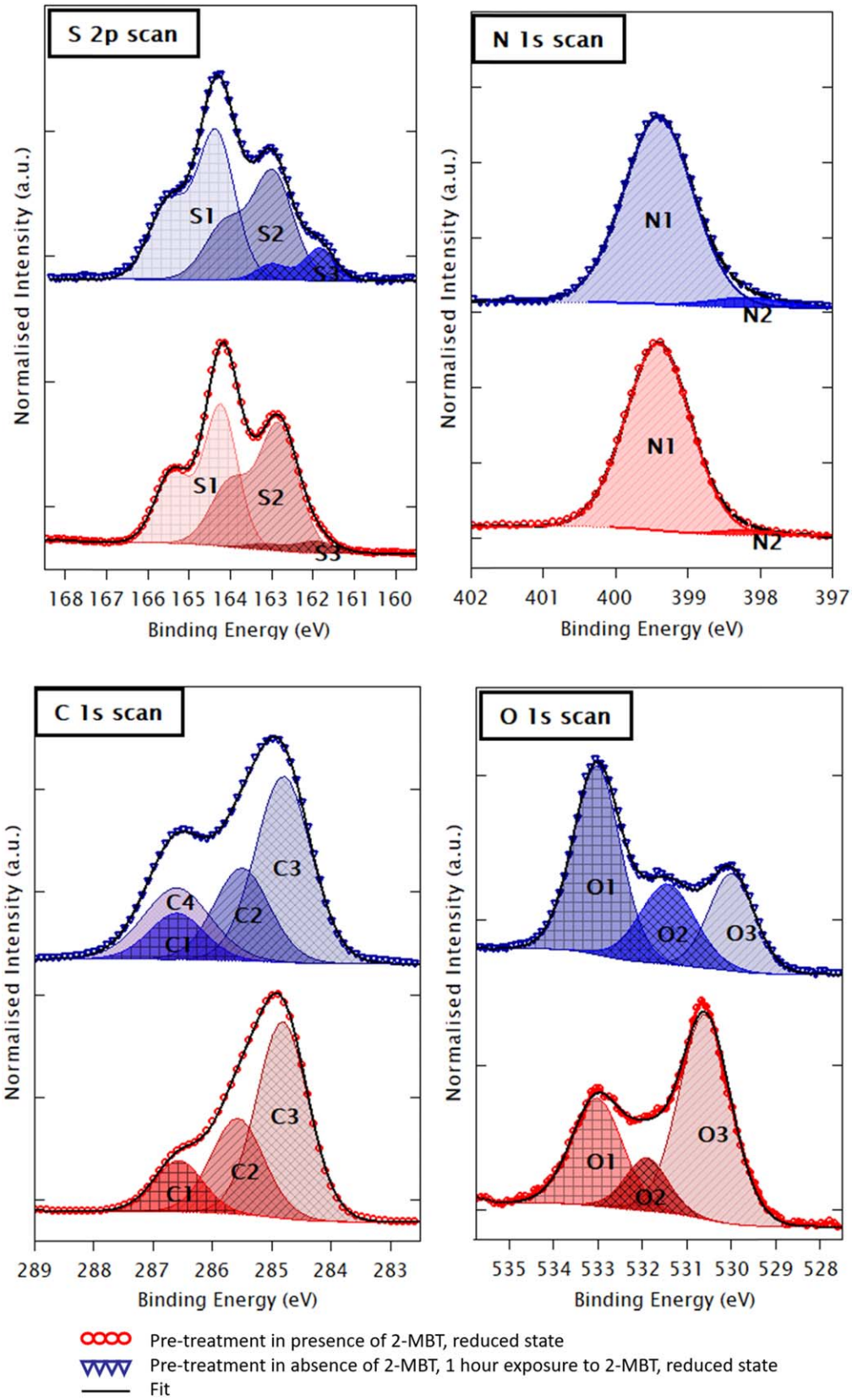

Figure 6. XPS S 2p, N 1s, C 1s, and O1s core level spectra of copper exposed to 0.1 M NaOH +1 mM 2-MBT solution in reduced state after pre-treatment in presence of 2-MBT (red curves), and pre-treatment in absence of 2-MBT followed by 1 h exposure to 2-MBT (blue curves).

on the top-most surface above the 2-MBT layer. Nonetheless, we cannot completely exclude the possibility of formation of a low quantity of alcohols (oxygen bonded to one carbon atom) or a slightly increased oxygen adsorption on the surface.

Regarding the line shape of the N 1s and S 2p spectra shown in Fig. 6, they are similar after either pre-treatment method which indicates resembling structures of the 2-MBT layers formed, despite the differences in thickness and in oxide quantities on the surface discussed above. In both cases, it is mostly the sulphur atoms that bond to metallic copper, as evidenced from the S3 peak in the S 2p spectrum and the ToF-SIMS depth profiles, like observed in acidic environment.[15] Only a tiny fraction of the nitrogen atoms bonds directly to the metallic copper here, which is shown by the presence of a peak at 398.2 eV in both N 1s spectra.[20]

Interface structure and composition.—In order to quantify the effect of the pre-treatment methods on the reduction of the native oxide film and formation of the 2-MBT barrier layers on the surface before and after anodic polarization, the photoelectron intensities of the elemental components obtained by spectral decomposition of the Cu 2p, N 1s, S 2p, and O 1s core levels were used as inputs in a model of photoelectron intensity attenuation (Fig. 7) previously developed[15] in order to estimate the thickness and coverage of Cu_2O oxide remaining at the interface and the thickness of the covering 2-MBT organic layer. In this model, detailed in Supplementary Information (SI), the oxide islands are assumed to have uniform thickness, and the covering organic layer to have the same surface flatness as the substrate. The values are estimated by numerically solving the system of equations given in SI, as well as calculation details. Despite the limitations of the model regarding the assumptions listed in SI and the high uncertainties on the coverage (±10%) and thickness (±0.2 nm) estimates, determined by the propagation of uncertainty, it remains an effective tool for comparison since enabling us to quantify differences between the differently prepared interfaces. The results for the present work are compiled in Table II. The equivalent thickness of the oxide was calculated by weighing its thickness with its coverage, and the equivalent thickness of the 2-MBT layer was calculated by combining the products of thickness and coverage of the 2-MBT layer on the metallic surface and on the oxidized surface, for ease of comparison.

Table II shows that the pre-treatment in absence of 2-MBT followed by 1 h exposure to the inhibitor results in low amounts of oxide remaining on the Cu surface. This is in agreement with the electrochemical CV data, ToF-SIMS depth profiles and Cu LMM Auger spectra. The coverage of the oxide islands is relatively high, 77% for the reduced state, and the thickness is estimated to be approximately 0.3 nm. The 2-MBT layer here is approximately 1.2 nm in equivalent thickness. In the anodic state of the surface, the coverage of oxide islands decreases marginally with their thickness remaining constant. It is proposed that during polarization, the ultra-thin Cu_2O oxide islands decompose, thus providing Cu atoms for the 2-MBT molecules to then bond with and thus increase the coverage of metallic Cu. The other hypothesis is that in the reduced state, there are regions of the surface not covered by the 2-MBT layer at all, which oxidize when in contact with air during sample transfer, thus giving a higher apparent coverage of oxide islands in this state. Upon anodic polarization, these uncovered regions would be oxidized to Cu(I) state, as suggested by the CV data, masking the artefact effects of air transfer. Regarding the 2-MBT layer, we observe a slight increase in the thickness after anodic polarization of the surface. This is discussed in detail later.

For the surface in reduced state after cathodic pre-treatment in the presence of 2-MBT, the initial coverage of the residual oxide islands is found lower, but their thickness approximately three times compared to the previous case due to either incomplete reduction of the native oxide film, as discussed earlier, or further oxidation of those regions during transfer of the samples through air. Although the coverage of the oxide islands in the reduced state is only around 54% of the surface, their thickness is estimated to be approximately 0.9 nm, indicating 3D oxide islands partially covering the Cu substrate. The 2-MBT organic layer is markedly thicker compared to the oxide islands, with an equivalent thickness of approximately 2.8 nm. This confirms our hypothesis of the formation of thicker organic multilayers as inferred from the ToF-SIMS data, and in agreement with previous work in acidic environment.[15]

Figure 7. Schematic of the bi-layer model used to estimate the thickness and coverage of the thin-layers covering the copper substrate.

Upon polarization, a moderate fraction of the surface is further oxidized, resulting in a higher coverage of the oxide islands while thickness is unchanged considering the experimental uncertainty. This supports residual anodic oxidation occurring mostly in the more reactive local areas of the interface initially with no subsisting native oxide film after pre-treatment. The trend for the thickness increase of the 2-MBT layer in the anodic state is observed in this case as well, from 2.77 to 2.97 nm (Table II). It is proposed that during anodic polarization, the 2-MBT molecules interact with the Cu(I) ions released in the solution to form Cu-2-MBT complexes that deposit on the surface and thus form a thicker organic layer, as evidenced in the ToF-SIMS depth profiles (Fig. 4). An indication of this is the difference between the anodic and cathodic charge densities during the cyclic voltammetry tests. As evidenced from Table I, there is a positive difference between the anodic and cathodic charge densities for all 4 experiments. Therefore, it is indisputable that there is some reacting Cu (from anodic charge) that is not involved in the growth of the oxide layer subsequently reduced (from cathodic charge). These excess Cu ions likely interact with the 2-MBT molecules to form the complexes and thus increase the thickness of the 2-MBT organic layer on the surface. In their work on corrosion inhibition of copper by 2-MBT, Ohsawa et al. concluded that it was indeed the Cu (I) ions that form complexes with the 2-MBT molecule.[16] This would also explain why we observe a thicker 2-MBT layer when there are more oxides on the copper surface in an alkaline environment (pre-treatment with 2-MBT) and why it increases upon polarization.

pH effects on interface.—Several authors have hypothesized that the formation of the 2-MBT layer on copper differs based on the environment and the initial surface oxidation state.[16,25,41] Since we have studied the adsorption of the 2-MBT inhibitor on Cu in acidic conditions in previous work,[15] we can now make a comparison with alkaline environment and discuss the differences in interface oxide layers and 2-MBT organic layers and try to understand why the changes in barrier layer formation occur.

It has been determined that in both environments, acidic and alkaline, the cathodic pre-treatment performed in absence of 2-MBT results in a nearly metallic state, whereas the pre-treatment performed in presence of 2-MBT results in a significant quantity of oxides unreduced. This indicates that in both environments there is an interaction between the 2-MBT molecules and copper oxide which then hampers the complete reduction of the native oxides present on the surface. Additionally, in both cases, the remaining oxides are trapped between the 2-MBT layer and the metallic substrate in the form of islands, instead of a fully covering layer.

Despite these similarities in the two environments, it was revealed that the thickness of the 2-MBT organic layer is larger on a relatively oxide free surface in the acidic environment, whereas it is the other way around in the alkaline environment, with a thicker 2-MBT layer observed in case of larger oxide quantities. Moreover, upon anodic polarization, a decrease in the thickness of the 2-MBT layer was observed in the acidic environment, whereas the present

Table II. Coverage and thickness of the copper oxide islands and thickness of 2-MBT organic layer estimated from quantitative analysis of the XPS data. The uncertainty on the coverage was estimated to be ±10% and the uncertainty on the thicknesses was estimated to be ±0.2 nm.

Electrochemical conditions	Coverage of Cu_2O islands (%)	Thickness of Cu_2O islands (nm)	Equivalent thickness of Cu_2O (nm)	Thickness of 2-MBT layer above oxides (nm)	Thickness of 2-MBT layer on metallic Cu (nm)	Equivalent thickness of 2-MBT layer (nm)
Pre-treatment w/o 2-MBT, 1 h exposure to 2-MBT, reduced state.	77	0.31	0.24	1.11	1.42	1.18
Pre-treatment w/o 2-MBT, 1 h exposure to 2-MBT, anodic state.	72	0.31	0.22	1.42	1.73	1.51
Pre-treatment with 2-MBT, reduced state	54	0.89	0.48	2.36	3.25	2.77
Pre-treatment with 2-MBT, anodic state	72	0.80	0.58	2.75	3.55	2.97

work shows that the 2-MBT layer increases in thickness in the alkaline environment. This difference is likely due to the conformer of the 2-MBT molecule that is stable in each environment. In the alkaline environment, the molecule, of which pK_a is 6.9,[49] would predominantly be in the thiolate form due to the excess OH^- ions present in the solution.[24] The deprotonation of the molecule offers an additional reactive site (N atom) in the molecule which increases the bonding possibilities with copper metal and copper oxides, as shown by DFT calculations,[26,50] and thus could promote the adsorption of 2-MBT molecules on the metallic substrate, increasing its coverage, and the formation of Cu-2-MBT complexes which then deposit on the surface, increasing the thickness of the organic layer. However, this is not the case in acidic environment where the molecule predominates in its protonated thione form Ref. 24 due to the excess H^+ ions in the solution, thus not offering an extra reactive site and limiting the possibilities of adsorbed configurations and bonding with copper metal and copper oxide. The presence of chloride ions in the HCl acidic environment could also have effects that are not seen in the NaOH alkaline environment studied here. The adsorption of Cl^- ions would be rather competitive with the adsorption of 2-MBT on copper, thus limiting the adsorption of the 2-MBT molecules and the growth of the organic layer. However, in the alkaline environment the 2-MBT layer is allowed to grow more freely without the influence of the aggressive chloride ions, which could possibly be a reason for the thicker organic layer in this case.

Regardless of the growth mechanism of the 2-MBT layer on the surface, the bonding between the molecules and the surface remains largely similar. In both strongly acidic and strongly alkaline conditions, the 2-MBT molecules bond with metallic copper mostly via their sulphur atoms. In the strongly alkaline conditions, a small fraction of N bonds directly to the metallic copper which most likely occurs due to the additional reactive sites formed by deprotonation of the molecule in the NaOH solution, as mentioned above. However, we can neither confirm nor exclude the possibility that there is an interaction between the copper oxides and the sulphur and/or nitrogen atoms of the molecule, like shown by DFT calculations.[26] This remains as one of the major questions yet to be dealt with.

Conclusions

The adsorption of the 2-MBT organic corrosion inhibitor and its effects on the anodic oxidation of copper in an alkaline environment were investigated by electrochemical and surface analytical techniques. It was shown that the formation of the 2-MBT layer on the surface impedes the growth of anodic oxide in the Cu(I) potential range. However, the presence of native oxide on the surface plays a major role in the formation and subsequent effectiveness of the organic layer as a barrier against anodic activity. Reduction of the native oxide film by cathodic pre-treatment performed in the absence of 2-MBT in the solution resulted in a nearly metallic state of the surface, whereas an incomplete reduction of the native oxide film was observed in the presence of 2-MBT, owing to the adsorption of 2-MBT on copper oxide and therefore blocking electro-reduction. The resulting organic barrier layer was substantially thicker compared to a surface with negligible oxides and included metal-organic complexes. This thicker 2-MBT barrier layer was more effective in impeding the growth of oxides upon anodic polarisation. Longer exposure times to the inhibitor of a surface with negligible oxides increased the efficiency of the organic barrier layer in impeding the growth of anodic oxide.

The organic barrier layer is multi-layered with the inner layer bonded to the copper substrate principally via the sulphur atoms of the molecules, as determined from the XPS spectra and the ToF-SIMS depth profiles. Additionally, a limited fraction of the nitrogen molecule is also bonded directly to the metallic substrate. The interaction between the copper oxides and the sulphur and/or nitrogen atoms from the molecules could not be resolved. Upon anodic polarisation, the 2-MBT barrier layer grows in thickness, with inclusion of Cu-2-MBT complexes. It is proposed that the thiolate form of 2-MBT, which is the dominant conformer in an alkaline environment, allows for additional bonding possibilities to the Cu atoms and Cu(I) ions released from the surface oxide, forming Cu-2-MBT complexes that deposit on the surface and thus increase the thickness of the organic barrier layer.

Acknowledgments

This project has received funding from the European Research Council (ERC) under the European Union's Horizon 2020 research and innovation program (ERC Advanced grant no. 741123).

The ToF-SIMS equipment has been partially funded by Région Ile-de-France.

ORCID

Vishant Garg https://orcid.org/0009-0006-0023-7755
Antoine Seyeux https://orcid.org/0000-0002-3062-8961
Frédéric Wiame https://orcid.org/0000-0002-1422-6858
Vincent Maurice https://orcid.org/0000-0001-5222-9972
Philippe Marcus https://orcid.org/0000-0002-9140-0047

References

1. E. Touzé and C. Cougnon, *Electrochim. Acta*, **262**, 206 (2018).
2. Y. Feng, K.-S. Siow, W.-K. Teo, K.-L. Tan, and A.-K. Hsieh, *Corrosion*, **53**, 389 (1997).
3. N. Takeno, *Geological survey of Japan open file report 419* (2005).
4. J. Ambrose, R. G. Barradas, and D. W. Shoesmith, *J. Electroanal. Chem. Interfacial Electrochem.*, **47**, 47 (1973).
5. B. Miller, *J. Electrochem. Soc.*, **116**, 1675 (1969).
6. H.-H. Strehblow and B. Titze, *Electrochim. Acta*, **25**, 839 (1980).
7. V. Maurice, H.-H. Strehblow, and P. Marcus, *Surf. Sci.*, **458**, 185 (2000).
8. J. Kunze, V. Maurice, L. H. Klein, H. H. Strehblow, and P. Marcus, *J. Phys. Chem. B*, **105**, 4263 (2001).
9. J. Kunze, V. Maurice, L. H. Klein, H. H. Strehblow, and P. Marcus, *Corros. Sci.*, **46**, 245 (2004).
10. V. Maurice, H.-H. Strehblow, and P. Marcus, *J. Electrochem. Soc.*, **146**, 524 (1999).
11. F. Wiame, V. Maurice, and P. Marcus, *Surf. Sci.*, **601**, 1193 (2007).
12. M. R. Pinnel, H. G. Tompkins, and D. E. Heath, *Appl. Surf. Sci.*, **2**, 558 (1979).
13. P. Marcus, V. Maurice, and H. H. Strehblow, *Corros. Sci.*, **50**, 2698 (2008).
14. H. Parangusan, J. Bhadra, and N. Al-Thani, *Emergent Mater*, **4**, 1187 (2021).
15. V. Garg, S. B. Sharma, S. Zanna, A. Seyeux, F. Wiame, V. Maurice, and P. Marcus, *Electrochim. Acta*, **447**, 142162 (2023).
16. M. Ohsawa and W. Suetaka, *Corros. Sci.*, **19**, 709 (1979).
17. E. Vernack, S. Zanna, A. Seyeux, D. Costa, F. Chiter, P. Tingaut, and P. Marcus, *Corros. Sci.*, **210**, 110854 (2023).
18. M. Finšgar and D. Kek Merl, *Corros. Sci.*, **83**, 164 (2014).
19. R. Woods, G. A. Hope, and K. Watling, *J. Appl. Electrochem.*, **30**, 1209 (2000).
20. X. Wu, F. Wiame, V. Maurice, and P. Marcus, *Corros. Sci.*, **166**, 108464 (2020).
21. X. Wu, F. Wiame, V. Maurice, and P. Marcus, *Corros. Sci.*, **189**, 109565 (2021).
22. X. Wu, F. Wiame, V. Maurice, and P. Marcus, *J. Phys. Chem. C*, **124**, 15995 (2020).
23. A. K. Rai, R. Singh, K. N. Singh, and V. B. Singh, *Spectrochim Acta A Mol Biomol Spectrosc*, **63**, 483 (2006).
24. B. Ellis and P. J. F. Griffiths, *Spectrochim. Acta*, **22**, 2005 (1966).
25. D. Chadwick and T. Hashemi, *Surf. Sci.*, **89**, 649 (1979).
26. F. Chiter, D. Costa, V. Maurice, and P. Marcus, *Appl. Surf. Sci.*, **537**, 147802 (2021).
27. F. Chiter, D. Costa, V. Maurice, and P. Marcus, *Npj. Mater. Degrad*, **7**, 5 (2023).
28. Y. S. Tan, M. P. Srinivasan, S. O. Pehkonen, and S. Y. M. Chooi, *J. Vac. Sci. Technol. A*, **22**, 1917 (2004).
29. S. B. Sharma, V. Maurice, L. H. Klein, and P. Marcus, *J. Electrochem. Soc.*, **167**, 161504 (2020).
30. S. B. Sharma, V. Maurice, L. H. Klein, and P. Marcus, *J. Electrochem. Soc.*, **168**, 061501 (2021).
31. M. Bettayeb, V. Maurice, L. H. Klein, L. Lapiere, K. Verbeken, and P. Marcus, *Electrochim. Acta*, **305**, 240 (2019).
32. S. Mirhashemihaghighi, J. Światowska, V. Maurice, A. Seyeux, L. H. Klein, E. Härkönen, M. Ritala, and P. Marcus, *J. Electrochem. Soc.*, **162**, C377 (2015).
33. J. H. Scofield, *J Electron Spectros Relat Phenomena*, **8**, 129 (1976).
34. H. Shinotsuka, S. Tanuma, and C. J. Powell, *Surf. Interface Anal.*, **54**, 534 (2022).
35. J. W. Diggle, T. C. Downie, and C. W. Goulding, *Chem. Rev.*, **69**, 365 (1969).
36. P. Visser, H. Terryn, and J. M. C. Mol, *Corros. Sci.*, **140**, 272 (2018).
37. H.-H. Strehblow, V. Maurice, and P. Marcus, *Electrochim. Acta*, **46**, 3755 (2001).
38. H. Chen et al., *J. Solid State Electrochem.*, **19**, 3501 (2015).
39. R. Subramanian and V. Lakshminarayanan, *Corros. Sci.*, **44**, 535 (2002).
40. I. A. Arkhipushkin, Y. E. Pronin, S. S. Vesely, and L. P. Kazansky, *Int J Corros Scale Inhib*, **3**, 078 (2014).
41. L. P. Kazansky, I. A. Selyaninov, and Y. I. Kuznetsov, *Appl. Surf. Sci.*, **258**, 6807 (2012).

42. F. Wiame, F. R. Jasnot, J. Światowska, A. Seyeux, F. Bertran, P. Le Fèvre, A. Taleb-Ibrahimi, V. Maurice, and P. Marcus, *Surf. Sci.*, **641**, 51 (2015).
43. A. Galtayries and J. P. Bonnelle, *Surf. Interface Anal.*, **23**, 171 (1995).
44. J. F. Moulder, W. F. Stickle, P. E. Sobol, K. D. Bomben, and J. Chastain, *Handbook of X-ray Photoelectron Spectroscopy: A Reference Book of Standard Spectra for Identification and Interpretation of XPS Data*, ed. J. Chastain (Waltham)(Perkin-Elmer Corporation) (1992).
45. D. Briggs and G. Beamson, *Anal. Chem.*, **64**, 1729 (1992).
46. G. Deroubaix and P. Marcus, *Surf. Interface Anal.*, **18**, 39 (1992).
47. W. Kautek and J. G. Gordon, *J. Electrochem. Soc.*, **137**, 2672 (1990).
48. D. Briggs and G. Beamson, *Anal. Chem.*, **65**, 1517 (1993).
49. J. P. Danehy and K. N. Parameswaran, *J. Chem. Eng. Data*, **13**, 386 (1968).
50. F. Chiter, D. Costa, V. Maurice, and P. Marcus, *Corros. Sci.*, **209**, 110658 (2022).